Journal
Nanoscience and Nanotechnology
Vol. 8, 4666–4669, 2008

RESEARCH ARTICLE

Study of the Magnetic Phase of Fe-Pt Alloy Nanoparticles

Hyungil Cha[1], Younghwan Kim[2], Changwoo Kim[1], and Youngsoo Kang[1,*]

[1] *Department of Chemistry, Sogang University, Seoul 121-742, Korea*
[2] *Department of Chemistry, Pukyong National University, Busan 608-737, Korea*

High temperature solution phase decomposition of $Fe(CO)_5$ and reduction of $Pt(acac)_2$ in the presence of stabilizers of oleic acid and oleyl amine are employed to produce $Fe_{1-x}Pt_x$ alloy nanoparticles. The Fe and Pt composition of the nanosized materials can be tuned by adjusting the molar ratio of $Fe(CO)_5$ to $Pt(acac)_2$, and the compositions ranging from $Fe_{40}Pt_{60}$ to $Fe_{80}Pt_{20}$ are obtained. This study is to investigate the influence of the composition on Curie temperature (T_c) of $Fe_{1-x}Pt_x$ nanoparticles monitored by thermomagnetic analysis (TMA).

Keywords: Solution Phase Decomposition, $Fe_{1-x}Pt_x$ Nanoparticles, Curie Temperature (T_c).

1. INTRODUCTION

Magnetic nanoparticles with sizes ranging from 2 to 20 nm in diameter represent an important class of artificial nanostructured materials. Their magnetic properties change drastically with their size, as the relaxation of the magnetization orientation of each particle is determined by $\tau = \tau_0 e^{KV/2\kappa T}$, in which s is the relaxation time at one orientation, K is the particle's anisotropy constant, V is the particle volume, κ is Boltzmann's constant, and T is temperature.[1,2] The term KV was measured as the energy barrier between two orientations. As the size of the particle decreases to a level where KV becomes comparable to the thermal energy κT, its magnetization starts to fluctuate from one direction to another. As a result, at this T the overall magnetic moment of this particle is randomized to zero, and the particle is said to be superparamagnetic.

The FePt compound with the tetragonal $L1o$-type structure; space group *P4/mmm* are of fundamental interest because their magnetic anisotropy based on $3d$ and $5d$ electrons is as large as that of the well-known rare earth transition metal high performance magnets based on the $3d$–$4f$-systems.[3–5] The large magnetic anisotropy of the $3d$–$5d$ ferromagnets is due to the large spin-orbit coupling in the $5d$-element. Magnets made of the $L1o$ phase have attracted much attention recently because of their potential usage in ultra high-density data storage[6] and permanent magnets for special applications. Distinct advantages of these compounds are, as opposed to the performance magnets, that they are very ductile and chemically inert. Self-organized magnetic arrays of dispersed $L1o$ particles (diameter ~10 nm) are expected to be superparamagnetic only at elevated temperature. Therefore they are considered as candidates for future thermally stable magnetic recording media with densities as high as 1 Tbit/in^2.[7] The understanding and the control of magnetocrystalline anisotropy energy in Fe-Pt alloy nanoscale building blocks is a crucial task to design new devices with desired magnetic properties.

According to the Fe-Pt phase diagrams in Figure 1(a), close to equiatomic Fe-Pt alloys exhibit a typical disordered transformation from the disordered face-centered cubic A1-type structure with low magnetic anisotropy when the temperature is lowered below 1300 °C and 825 °C, respectively.[8] Unfortunately, it is not evident that bulk properties can be directly applied to nanoparticles systems. Curie temperature (T_c) is one of the widely used to determine magnetic phase. At temperatures below the T_c, the magnetic moments are partially aligned within magnetic domains in ferromagnetic materials. As the temperature is increased from below the T_c, thermal fluctuations increasingly destroy this alignment, until the net magnetization becomes zero at and above the T_c. Above T_c, the material is purely paramagnetic. Herein we report an experimental determination of the T_c for different compositions.

2. EXPERIMENTAL DETAILS

$Fe(CO)_5$, $Pt(acac)_2$, oleylamine, and benzyl ether were purchased from Aldrich Chemical Co.; Oleic acid was purchased from Junsei Chemical Co. Ltd. Ethanol and cyclohexane were purchased from Fisher Scientific. To prepare monodispersed $Fe_{1-x}Pt_x$ magnetic nanoparticles by

---

[*] Author to whom correspondence should be addressed.

1533-4880/2008/8/4666/004 doi:10.1166/jnn.2008.IC16

---

the high te
Fe(CO)5 ar
oleylamine,
elsewhere.[9]
were contro
cursors. Th
the forming
persed in h
To deterr
studies wer
microscope
pared by d
A drop was
on a coppe
ination was
20 kV for s
Elemental a
energy disp
JEM2010 I
age of 200
made using
using a mic
tioned belo
a thermo-m
TGA 7) cu
sus temper
(10 °C/min
(10 °C/min
same condi
tion has gi
363 ± 2 °C
netic prope
a supercon
MPMS XL

3. RESU

Interesting
atomic per
magnetic n
ically diso
chemically
as shown i
The fcc-
magnetical
can be vie
stacked alo
The aim c
ence of th
cles. The c
responsibl
increasing
and finite-
The na
compositio
with a sta

high temperature solution phase decomposition of (CO)$_5$ and Pt(acac)$_2$ in the presence of oleic acid, eylamine, and benzyl ether as solvent as described sewhere.[9] The composition of the $Fe_{1-x}Pt_x$ nanoparticles re controlled by turning the molar ratio the metal prersors. The resulting solution was dried and resulted in forming of an air-stable powder, which could be redisrsed in hexane at any concentration.

To determine the size distribution of the particles, TEM udies were carried out using HITACHI H-7500 electron microscope operated at 80 kV. TEM specimens were prered by dropping particle solution on the copper grid. drop was poured onto a porous carbon film supported n a copper grid, then slowly evaporated. FE-SEM examation was performed in JEOL JSM 6700F operating at 0 kV for structure and shape of FePt alloy nanoparticles. lemental analysis of the sample was performed by using ergy dispersive X-ray microanalysis (EDX) on a JEOL EM2010 FE-SEM operated under an acceleration voltge of 200 kV. Curie temperature (T_c) measurements were ade using temperature scans of the thermo-gravimetry sing a microbalance with a magnetic field gradient positioned below the sample was used for the measurement of thermo-magnetic analysis (TMA, Perkin-Elmer (U.S.A), GA 7) curve showing the downward magnetic force veris temperature. Sample was heated from 50 to 850 °C 0 °C/min) and cooled from 850 °C to 50 °C occurred 0 °C/min). The applied field was $\mu_o H = 6$ mT. Under the me conditions, a pure Fe standard used for the calibraon has given $T_c = 770 \pm 1$ °C and pure Ni standard $T_c =$ 63 ± 2 °C (an average of three measurements). The magetic properties of the nanoparticles were studied using superconducting quantum interference device (SQUID, PMS XL 7) magnetometer.

RESULTS AND DISCUSSION

terestingly, FePt nanoparticles containing a near-equal omic percentage of Fe and Pt are an important class of gnetic nanomaterials. They are known to have a chemlly disordered face-centered cubic (fcc) structure or a emically ordered face-centered tetragonal (fct) structure, shown in Figure 1.[10]

The fcc-structured FePt has a small coercivity and is gnetically soft. The fully ordered fct-structured FePt n be viewed as alternating atomic layers of Fe and Pt cked along the [001] direction (the c-axis in Fig. 1(c)). e aim of the present study is to investigate the influce of the composition on the T_c of $Fe_{1-x}Pt_x$ nanoparties. The contribution of the orbital magnetism, which is ponsible for the T_c, is found to change as a function of easing Pt contents, indicating the importance of surface finite-size effects in these composite of nanoparticles. The nanoparticles exhibit spherical morphology, for mpositions $Fe_{56}Pt_{44}$. The mean particle diameter is 8 nm a standard deviation of 0.6 nm. In Figure 2 we show one example of many TEM microscopes for $Fe_{56}Pt_{44}$ that presents nanoparticles.

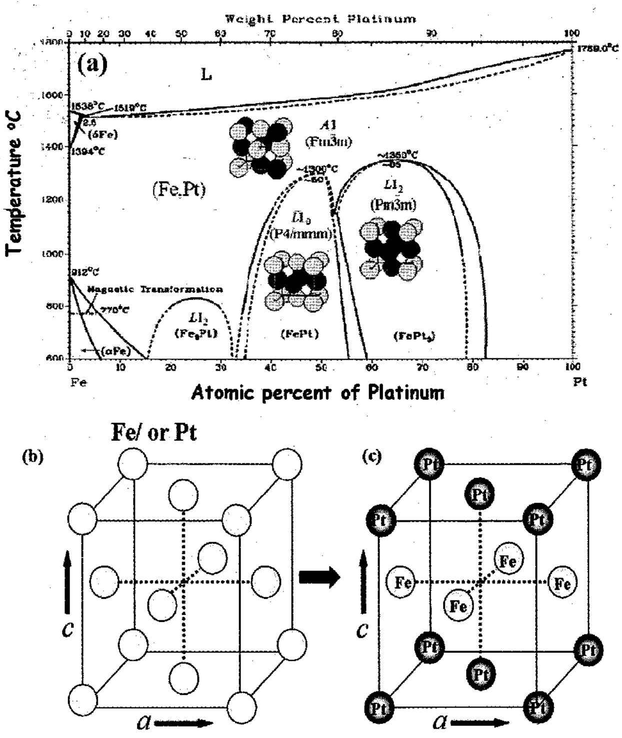

Fig. 1. Equilibrium phase (a) of the Fe-Pt system shown schematically are crystallographic structures of the phases in the corresponding phase equilibrium regions. Schematic illustration of the unit cell of (b) chemically disordered fcc, and (c) chemically ordered fct FePt.

Figure 3 shows the FE-SEM images of each $Fe_{1-x}Pt_x$ nanoparticles with various compositions. The

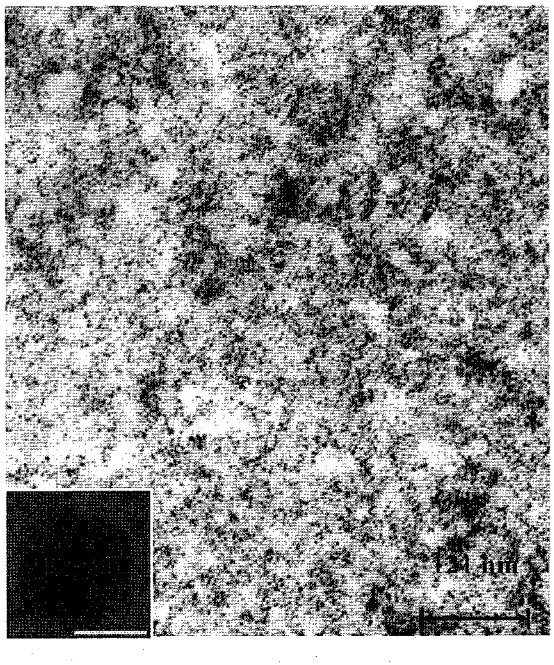

Fig. 2. TEM micrograph of the $Fe_{56}Pt_{44}$ nanoparticles dried on a conventional TEM grid. The inset shows spherical nanoparticle. Scale bar is 5 nm.

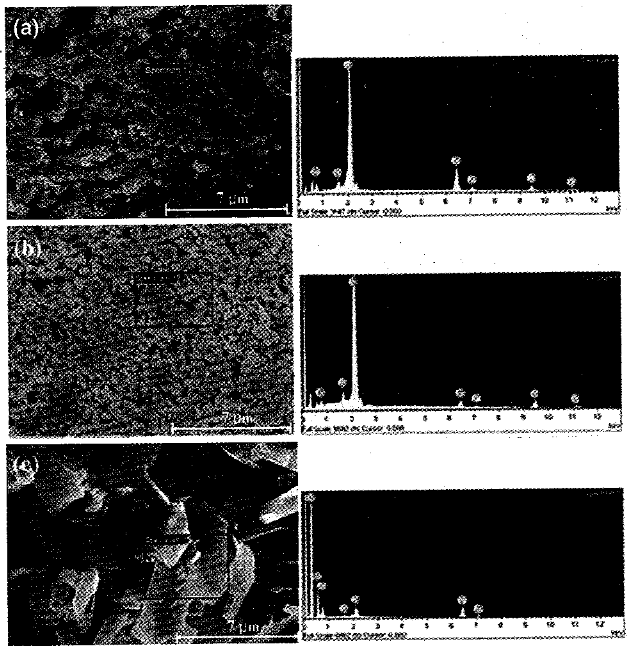

Fig. 3. FE-SEM images and energy dispersive X-ray microanalysis (EDX) of $Fe_{1-x}Pt_x$ nanoparticles; (a) $Fe_{56}Pt_{44}$, (b) $Fe_{40}Pt_{60}$, and (c) $Fe_{87}Pt_{13}$.

morphologies heavily depend on the composition of $Fe_{1-x}Pt_x$ nanoparticles. Table I summarizes the variation.

For the $Fe_{56}Pt_{44}$ and $Fe_{40}Pt_{60}$ products, the particles size distributions are narrow (10–25 nm) and spherical particles are obtained. When the Pt content is decreased, as found for $Fe_{87}Pt_{13}$, the particle size distributions are broadened and change the spherical to octahedral morphology collapses.

With the variation of the composition ratio, the morphology of the $Fe_{1-x}Pt_x$ changed. Also, energy dispersive X-ray analyses (EDX) in the FE-SEM measurements were performed to determine the chemical compositions of the $Fe_{1-x}Pt_x$ nanoparticles. A detailed statistical analysis of the EDX spectra recorded for many particles showed that the nominal $Fe_{54}Pt_{46}$, $Fe_{40}Pt_{60}$, and $Fe_{87}Pt_{13}$ particle composition varied by up to 3% around the nominal composition (Table I).

$Fe_{1-x}Pt_x$ nanoparticles were subjected to the TMA. The obtained TMA data were plotted in Figure 4. We find that the T_c for the $Fe_{1-x}Pt_x$ nanoparticles depend curvedly on composition as predicted. As decreasing Pt contents, the T_c increased except a near-equal atomic percentage of Fe and Pt. This range cause chemically ordered fct FePt nanoparticles during TMA measurement.

Table I. Composition of the $Fe_{1-x}Pt_x$ nanoparticles.

Molar ratio of $Fe(CO)_5$:$Pt(acac)_2$	(a) 2:1	(b) 2:3	(c) 3:2
Chemical composition	55.52:44.48	39.62:60.08	87.67:12.33

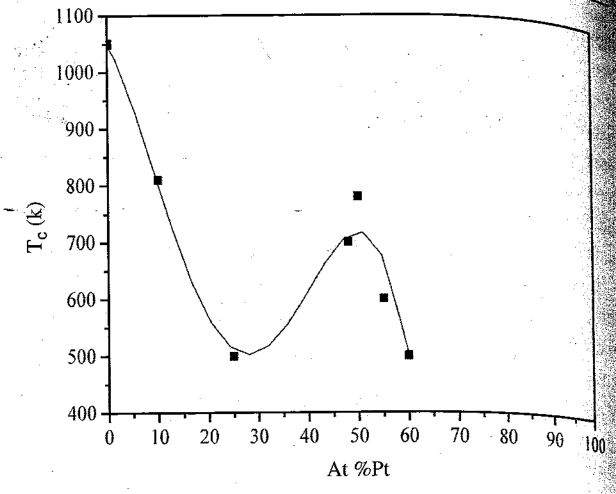

Fig. 4. Room temperature magnetic hysteresis loop of T_c measured $Fe_{1-x}Pt_x$ nanoparticles; (a) $Fe_{56}Pt_{42}$, (b) $Fe_{40}Pt_{60}$, and (c) $Fe_{87}Pt_{13}$.

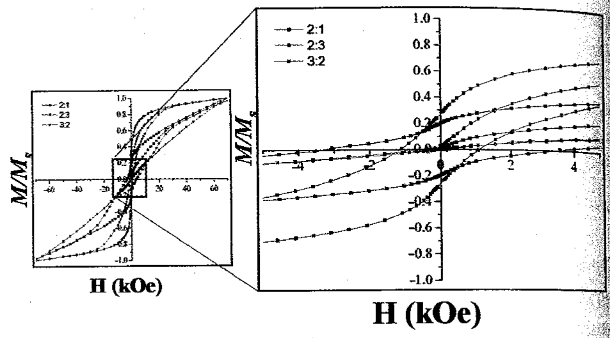

Fig. 5. Plotted T_c values of each of $Fe_{1-x}Pt_x$.

The magnetic properties of $Fe_{1-x}Pt_x$ nanoparticles were studied by hysteresis loop of SQUID at room temperature after TMA measurement in Figure 5. The coercivities of the $Fe_{1-x}Pt_x$ nanoparticles at room temperature are determined as 3.8, 1.3, and 0.08 kOe. A decreasing tendency of coercivity is good agreement with Gaussian type as described elsewhere.[11]

4. CONCLUSION

In conclusion, by monitoring T_c experiment we have shown that the T_c and coercivity of $Fe_{1-x}Pt_x$ nanoparticles increases as a function of decreasing Pt content except a near-equal atomic percentage of Fe and Pt. It is demonstrated that T_c for the $Fe_{1-x}Pt_x$ nanoparticles depend curvedly on composition. Although more work is needed, there are promising fundamental knowledge to understand and the control of Curie temperature in Fe-Pt alloy nanoscale building blocks in order to design new devices with desired magnetic properties.

Acknowledgments: Thank Dr. Sun Bae Kang at the Cooperative Lab. Center of Pukyong National University for assisting in the TEM and FE-SEM measurements. This research was supported by the Program for the Training of Graduate Students in Regional Innovation which was conducted by the Ministry of Commerce, Industry and Energy of the Korean Government, Brain Korea 21 project in 2007 and Nano R&D Program (Korea Science and Engineering Foundation, Grant 2007-02628).

References and Notes

1. A. H. Morrish, The Physical Principles of Magnetism, Wiley, New York (**1965**), Chap. 7.
2. K. M. Unruh and C. L. Chien, Nanomaterials: Synthesis, Properties and Applications, edited by A. S. Edelstein and R. C. Cammarata, Institute of Physics Publishing, Bristol, UK (**1996**), Chap. 14.
3. R. Skomski and J. M. Coey, Permanent Magnetizm, IoP Publishing, Bristol (**1999**).
4. N. I. Vlasova, G. S. Kandaurova, and N. N. Shchegoleva, *J. Magn. Magn. Mater.* 222, 138 (**2000**).
5. O. A. Ivanov, L. V. Solina, V. A. Demshina, and L. M. Magat, *Phys. Metall. Metalloved* 222, 138 (**2002**).
6. S. Sun, C. B. Murray, D. Weller, L. Folks, and A. Moser, *Science* 287, 1989 (**2000**).
7. T. J. Klemmer, C. Liu, N. Shukla, X. W. Wu, D. Weller, M. Tanase, D. E. Laughlin, and W. A. Soffa, *J. Magn. Magn. Mater.* 266, 79 (**2003**).
8. O. Gutfleisch, J. Lyubina, K. H. Muller, and L. Schulta, *Adv. Eng. Mater.* 7, 208 (**2005**).
9. M. Chen, J. P. Liu, and S. Sun, *J. Am. Chem. Soc.* 126, 8394 (**2004**).
10. S. Sun, *Adv. Mater.* 18, 393 (**2006**).
11. S. Sun, E. E. Fullerton, D. Weller, and C. B. Murray, *IEEE Trans. Magn.* 37, 1239 (**2001**).

Received: 9 May 2007. Accepted: 20 September 2007.